NATIONAL AND KAPODISTRIAN UNIVERSITY OF ATHENS

SCHOOL OF SCIENCES
DEPARTMENT OF INFORMATICS AND TELECOMMUNICATIONS

BSc THESIS

Beam Management Strategies for Wireless Communications with Reconfigurable Intelligent Surfaces

Kalliopi Christina E. Despotidou

Supervisor: **George C. Alexandropoulos,** Associate Professor NKUA

ATHENS

SEPTEMBER 2024

ΕΘΝΙΚΟ ΚΑΙ ΚΑΠΟΔΙΣΤΡΙΑΚΟ ΠΑΝΕΠΙΣΤΗΜΙΟ ΑΘΗΝΩΝ

ΣΧΟΛΗ ΘΕΤΙΚΩΝ ΕΠΙΣΤΗΜΩΝ
ΤΜΗΜΑ ΠΛΗΡΟΦΟΡΙΚΗΣ ΚΑΙ ΤΗΛΕΠΙΚΟΙΝΩΝΙΩΝ

ΠΤΥΧΙΑΚΗ ΕΡΓΑΣΙΑ

Στρατηγικές Διαχείρισης Δέσμης σε Ασύρματες Επικοινωνίες με Έξυπνες Επαναδιαμορφώσιμες Επιφάνειες Μεταϋλικών

Καλλιόπη Χριστίνα Ε. Δεσποτίδου

Επιβλέπων: **Γεώργιος Χ. Αλεξανδρόπουλος,** Αναπληρωτής Καθηγητής ΕΚΠΑ

ΑΘΗΝΑ

ΣΕΠΤΕΜΒΡΙΟΣ 2024

BSc THESIS

Beam Management Strategies for Wireless Communications with Reconfigurable Intelligent Surfaces

Kalliopi Christina E. Despotidou

S.N.: 11152000045

SUPERVISOR: **George C. Alexandropoulos,** Associate Professor NKUA

ΠΤΥΧΙΑΚΗ ΕΡΓΑΣΙΑ

Στρατηγικές Διαχείρισης Δέσμης σε Ασύρματες Επικοινωνίες με Έξυπνες Επαναδιαμορφώσιμες Επιφάνειες Μεταϋλικών

Καλλιόπη Χριστίνα Ε. Δεσποτίδου

Α.Μ.: 11152000045

ΕΠΙΒΛΕΠΩΝ: Γεώργιος Χ. Αλεξανδρόπουλος, Αναπληρωτής Καθηγητής ΕΚΠΑ

ABSTRACT

As the demand for high-speed, reliable, and energy-efficient wireless communications continues to escalate, driven by the proliferation of connected devices and the rollout of 5G networks, new innovative technologies are essential. Reconfigurable Intelligent Surfaces (RIS) have emerged as a promising solution to enhance wireless communications by dynamically manipulating the propagation of electromagnetic waves. This approach offers a cost-effective, energy-efficient means to improve signal quality and coverage without relying on power-hungry transceivers and/or extensive network infrastructure.

This thesis focuses on the near-field beam management problem for RIS-assisted millimeter-wave (mmWave) multi-antenna systems. We analyze key experiments from recent studies on the topic, specifically exploring hierarchical RIS phase profile codebooks for beam control in near-field environments, which are characterized by shorter communication distances and complex propagation conditions. Such environments pose unique challenges requiring sophisticated signal alignment techniques, which RIS technology adeptly addresses by intelligently reflecting and directing signals.

Through the implementation of state-of-the-art algorithms and frameworks, this thesis evaluates the effectiveness of RIS-based beam alignment and phase-shift optimization for near-field wireless communications. Extensive simulations are conducted to assess how these techniques minimize the overhead associated with channel state information (CSI) acquisition while enhancing signal quality and the overall system performance. The results affirm that RIS, in conjunction with hierarchical codebooks, can efficiently manage beam control, leading to significant improvements in energy efficiency and signal coverage for mmWave wireless communication networks.

By thoroughly investigating and validating existing methodologies, this thesis not only contributes to the understanding of some key practical considerations of the RIS technology, but also provides valuable insights into its potential limitations and future directions. The thesis' findings emphasize the critical role of RIS in revolutionizing wireless communications, especially as society moves towards increasingly connected environments with the advent of 5G-Advanced, 6G, and the Internet of Things (IoT).

SUBJECT AREA: Wireless Communications, Signal Processing, Beam Management

KEYWORDS: Reconfigurable Intelligent Surfaces, Hierarchical Phase-Shift Codebooks, Multi-Antenna Systems, Channel State Information, Near-Field Propagation

ΠΕΡΙΛΗΨΗ

Η ζήτηση για γρήγορες, αξιόπιστες και ενεργειακά αποδοτικές ασύρματες επικοινωνίες αυξάνεται συνεχώς. Ολοένα και περισσότερες συσκευές συνδέονται στο διαδίκτυο και σε συνδυασμό με την ανάπτυξη των ασύρματων συστημάτων 5ης Γενιάς (5G) καθιστούν απαραίτητες νέες καινοτόμες τεχνολογίες για την αντιμετώπιση αυτών των προκλήσεων. Οι έξυπνες επαναδιαμορφώσιμες επιφάνειες μεταϋλικών (Reconfigurable Intelligent Surfaces (RIS)) αποτελούν μια πολλά υποσχόμενη λύση, η οποία αναμένεται να βελτιώσει αισθητά την ασύρματη επικοινωνία μέσω της δυναμικής διαχείρισης της διάδοσης των ηλεκτρομαγνητικών κυμάτων που υλοποιεί. Αυτή η προσέγγιση προσφέρει έναν οικονομικά και ενεργειακά αποδοτικό τρόπο βελτίωσης της ποιότητας του σήματος και της κάλυψης χωρίς να βασίζεται σε ενεργοβόρους πομποδέκτες ή/και ακριβή δικτυακή υποδομή.

Η προκείμενη πτυχιακή εργασία επικεντρώνεται σε προηγμένες τεχνικές διαχείρισης δέσμης για συστήματα πολλαπλών κεραιών mmWave που χρησιμοποιούν RIS. Συγκεκριμένα, αναλύονται διεξοδικά βασικά πειράματα από πρόσφατες μελέτες που εξερευνούν ιεραρχικά κωδικοβιβλία φάσης RIS (hierarchical RIS phase profile codebooks) για τον έλεγχο δέσμης σε περιβάλλοντα κοντινού πεδίου, τα οποία χαρακτηρίζονται από μικρότερες αποστάσεις επικοινωνίας και σύνθετες συνθήκες διάδοσης. Αυτά τα περιβάλλοντα επιβάλλουν σημαντικές προκλήσεις που απαιτούν προηγμένες τεχνικές ευθυγράμμισης δέσμης σήματος, τις οποίες η τεχνολογία RIS μπορεί να αντιμετωπίσει αποτελεσματικά, ανακλώντας και κατευθύνοντας τα σήματα στο χώρο.

Μέσω της υλοποίησης προσφάτως προτεινόμενων αλγορίθμων, η προκείμενη πτυχιακή εργασία αξιολογεί την αποτελεσματικότητα της ευθυγράμμισης δέσμης RIS και της βελτιστοποίησης της φάσης της επιφάνειας για επικοινωνίες κοντινού πεδίου. Διεξάγονται εκτενείς προσομοιώσεις για να αξιολογηθεί πώς αυτές οι τεχνικές ελαχιστοποιούν την επιβάρυνση που σχετίζεται με την εκτίμηση της κατάστασης του ασύρματου, ενώ βελτιώνουν την ποιότητα του σήματος και τη συνολική απόδοση του συστήματος. Τα αποτελέσματα επιβεβαιώνουν ότι οι RIS, σε συνδυασμό με ιεραρχικά κωδικοβιβλία φάσης, μπορούν να διαχειριστούν αποτελεσματικά τον έλεγχο της δέσμης, οδηγώντας σε σημαντικές βελτιώσεις στην ενεργειακή απόδοση και την κάλυψη σήματος σε ασύρματα δικτύα σε συχνότητες mmWave.

Μέσω της διερεύνησης των υφιστάμενων μεθοδολογιών, αυτή η εργασία δε συμβάλλει μόνο στην κατανόηση των πρακτικών εφαρμογών της τεχνολογίας RIS, αλλά επίσης παρέχει πολύτιμες πληροφορίες για τους πιθανούς περιορισμούς και τις μελλοντικές κατευθύνσεις της. Τα ευρήματα της πτυχιακής εργασίας τονίζουν τον κρίσιμο ρόλο των RIS στις μελλοντικές ασύρματες επικοινωνίες, ειδικά καθώς η κοινωνία προχωρά προς όλο και πιο διασυνδεδεμένα περιβάλλοντα με την άφιξη των δικτύων 5G-Advanced, 6G και του Διαδικτύου των Πραγμάτων (IoT).

ΘΕΜΑΤΙΚΗ ΠΕΡΙΟΧΗ: Ασύρματες Επικοινωνίες, Επεξεργασία Σήματος, Διαχείριση Δέσμης

ΛΕΞΕΙΣ ΚΛΕΙΔΙΑ: Έξυπνες Επαναδιαμορφώσιμες Επιφάνειες Μεταϋλικών, Ιεραρχικά Κωδικοβιβλία Φάσης, Συστήματα Πολλαπλών Κεραιών, Πληροφορίες Κατάστασης Καναλιού, Διάδοση Κοντινού Πεδίου

ACKNOWLEDGEMENTS

I would like to express my deepest gratitude to my supervisor, Professor George C. Alexandropoulos, for his guidance, support, and encouragement throughout this project. His expertise and insights were key in shaping the direction and content of this thesis. I'm incredibly grateful for the opportunities he provided that helped me grow academically.

I also wish to thank Panagiotis Gavriilidis, whose patience, dedication, and technical expertise were instrumental in developing and completing this work. His support in helping me understand complex concepts and navigate challenges was deeply appreciated.

Furthermore, I am grateful to the Department of Informatics and Telecommunications at the National and Kapodistrian University of Athens for offering a stimulating environment where I could explore my interests and expand my knowledge in wireless communications.

To my family and friends, thank you for your unwavering support, love, and encouragement during the completion of this work. Your belief in me kept me motivated through the most challenging times.

Lastly, I'd like to acknowledge all the researchers and contributors whose work has laid the foundation for this thesis and continues to inspire the future of wireless communication.

CONTENTS

LIST OF FIGURES

LIST OF TABLES

1. INTRODUCTION

Millimeter-wave (mmWave) communications have emerged as essential for beyond 5G (B5G) and future 6G systems, largely driven by the exponential rise in wireless data demand. While mmWave offers high data rates and large bandwidth, it faces critical challenges, including significant path loss and sensitivity to environmental blockages. To mitigate these issues, large antenna arrays and advanced beamforming techniques are utilized to improve signal strength and counteract degradation. At even higher frequencies, such as the THz band, additional complexities like beam squint and frequency selectivity, often worsened by molecular absorption, further degrade performance in multipath conditions [33]. In these scenarios, single-carrier (SC) transmission schemes have proven advantageous, providing resilience against high peak-to-average power ratios compared to traditional multi-carrier approaches, and enabling more robust channel estimation for extremely large (XL) MIMO systems. Reconfigurable Intelligent Surfaces (RIS) present an additional, promising solution to these challenges by dynamically shaping the wireless environment and offering adaptive beam management, thus enhancing mmWave and THz communications, especially in dense and complex environments.

1.1 The Technology of Reconfigurable Intelligent Surfaces (RISs)

The rapid advancements in wireless communications necessitate innovative approaches to manage complex propagation environments. A promising technology at the forefront of this innovation is the Reconfigurable Intelligent Surface (RIS), which introduces unprecedented flexibility in controlling the electromagnetic (EM) properties of wireless communication channels. RIS technology consists of arrays of passive reflecting elements that can be programmed to adjust their phase shifts, enabling precise control over how incoming signals are reflected and directed. By transforming traditionally passive environments into dynamic, interactive ones, RISs offer a unique method of managing wireless signal propagation, presenting new possibilities for achieving energy-efficient, high-throughput, and low-latency communication systems.

The potential of RIS technology is particularly evident in scenarios where traditional wireless approaches face limitations. Unlike conventional base stations and relays, which generate new signals for communication, RISs enable a ”smart radio environment” by recycling existing radio waves instead of creating new emissions, significantly reducing power consumption. This shift challenges the traditional ”more data needs more power” assumption, positioning RISs as key to building sustainable wireless systems [26].

In both indoor and outdoor settings, RISs can be seamlessly integrated onto surfaces like building facades, ceilings, and walls, transforming passive surroundings into intelligent elements that enhance signal transmission. This integration allows for higher coverage, greater throughput, and more resilient connections. Recent research has concentrated on optimizing RIS phase shifts and power allocation to maximize energy efficiency and meet user-specific requirements. Advanced algorithms using techniques such as alternating maximization, gradient descent, and sequential fractional programming have shown that RIS-based solutions can improve energy efficiency by up to 300% compared to traditional amplify-and-forward relaying methods [15].

RIS technology also presents new challenges and opportunities in system-level integration, requiring dedicated control mechanisms and signaling protocols. For example,

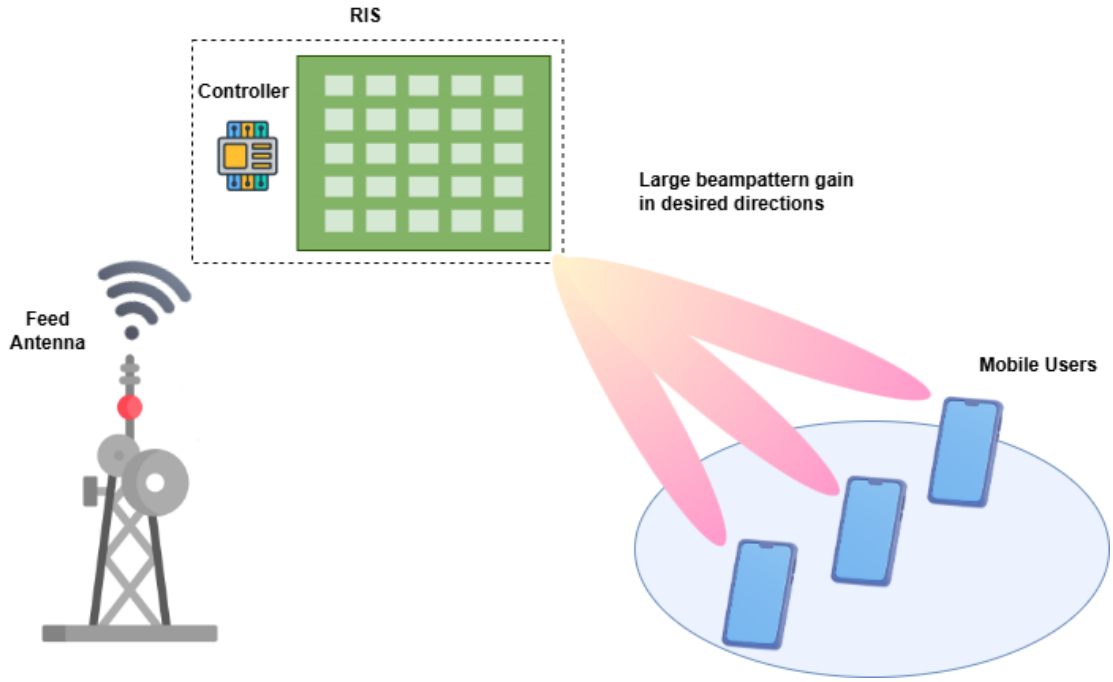

Figure 1.1: RIS-assisted beam management.

frameworks for managing RIS control operations consider the allocation of control channel bandwidth and rate selection, providing insight into the trade-offs between control overhead, channel estimation, and communication performance [27]. Hardware innovations have further propelled RIS feasibility, enabling cost-effective and scalable implementations that integrate with existing networks to create intelligent wireless environments [14].

1.2 The Beam Alignment Objective

Recent research on RISs has demonstrated their dual functionality in enabling simultaneous Passive Beamforming and Information Transfer (PBIT) through smart reflections [19]. This functionality is illustrated in an RIS-enhanced multiple-input single-output system employing Reflection Pattern Modulation (RPM) to achieve PBIT. In this system, active beamforming at the Access Point (AP) and passive beamforming at the RIS are jointly optimized to maximize the average received signal power, while taking into account communication outage probability. Leveraging the statistically known RIS state information at the AP, an alternating optimization method provides a high-quality suboptimal solution, along with a closed-form expression for the asymptotic outage probability under Rician fading. As a result, RIS-based systems using RPM can achieve significantly higher achievable rates than conventional systems without information transfer.

However, implementing RIS-assisted systems in the mmWave band presents substantial challenges in Channel State Information (CSI) acquisition, crucial for optimal beamforming. Unlike conventional systems, RIS cannot directly transmit or receive signals, complicating the acquisition of full CSI for both the Base Station-RIS (BS-RIS) and RIS-User links. Additionally, the large antenna arrays at both the base station and RIS, combined with the numerous passive elements, lead to considerable training overhead and computational complexity. Although Compressed Sensing (CS) techniques have been explored to simplify channel estimation by exploiting the sparse nature of mmWave channels, these methods often carry high computational costs, highlighting the need for efficient CSI ac-

quisition techniques in RIS-based systems.

Fortunately, the sparse scattering characteristic of mmWave channels presents an opportunity for more practical beam alignment (BA) techniques. In these environments, the line-of-sight (LOS) path typically dominates over non-line-of-sight (NLOS) components. A more efficient approach in such conditions is to identify and align the transmitter and receiver beams along the dominant path, maximizing signal strength. This BA process aims to identify optimal beam pairs; however, in RIS-assisted systems, BA becomes more complex since RIS cannot actively participate in signal transmission or reception. This limitation necessitates sophisticated methods to optimize beam alignment across both the BS-RIS and RIS-User links, ensuring that RIS can effectively contribute to overall system performance even without direct CSI acquisition capabilities.

This thesis focuses on near-field beam management techniques for RIS-enabled millimeter wave multi-antenna systems. The emergence of near-field communication (NFC) technologies represents a significant advancement in wireless communications, as these technologies leverage high-frequency signals for efficient data transfer over short distances [9, 11, 25, 39]. Recent studies indicate that such communication scenarios, characterized by shorter distances and specific propagation conditions, require advanced beamforming and signal alignment techniques to optimize performance. In this work, we replicate and analyze key experiments that explore hierarchical phase-shift codebooks for beam control in near-field environments, which present unique challenges that can significantly affect communication efficacy.

Reconfigurable Intelligent Surface (RIS) technology offers a promising solution by intelligently reflecting and directing signals, thereby enhancing overall system performance in these scenarios. Additionally, we evaluate the effectiveness of the proposed methods under varying Line-of-Sight (LOS) conditions, testing different values of the Ricean factor K_h—which represents the power ratio between LOS and Non-Line-of-Sight (NLOS) components—to assess the impact of LOS dominance on system performance. The findings underscore the critical role of RIS technology in shaping the future of wireless communication, particularly as society transitions towards more connected environments with the advent of 5G, 6G, and the Internet of Things (IoT) [22, 24, 32].

2. BACKGROUND AND RELATED WORK

2.1 RIS Architecture and Operational Modes

The advent of wireless connectivity empowered by Reconfigurable Intelligent Surfaces (RIS) represents a transformative technology within the rapidly evolving landscape of 6G mobile networks. As the demand for seamless and efficient wireless communications intensifies, RIS offer a compelling approach by actively manipulating the radio propagation environment to enhance connectivity. This section provides an overview of recent advancements in RIS technology, highlighting its architectural diversity and various operational modes.

Historically, the control of electromagnetic (EM) wave propagation has been a central design objective across many domains, including medical imaging and nanolithography. Approaches utilizing phase and/or amplitude control via reflect arrays, metamaterials, and spatial light modulators have paved the way for the development of RIS technology in wireless communications. A RIS is defined as a planar array of multiple ultrathin meta-atoms (also referred to as unit cells or elements), each possessing multiple digital states corresponding to distinct EM responses.

These tunable meta-atoms are an active area of research and can vary with the operating frequency. Examples include p-i-n diodes and varactors for millimeter-wave (mmWave) frequencies, and materials such as liquid crystals, graphene, vanadium dioxide, memristors, and microfluidics for THz applications. Initially, each tunable-state meta-atom was designed to contribute a phase shift to its impinging signal. The maintenance and alteration of a reflective meta-atom's state require minimal power consumption, managed by an active device known as the RIS controller, which also interfaces with the wireless network. This standard passive RIS structure, primarily reflective, illustrates the foundational concept of RIS.

Recent advancements have seen a growing interest in alternative RIS hardware architectures and multifunctional capabilities, addressing some limitations of passive designs while offering additional operational features. As emphasized in [8], RISs are pivotal in the evolution of 6G networks, offering a revolutionary approach to optimizing wireless communications. Understanding the foundational hardware components of RIS is essential for unlocking the full potential of this technology in next-generation networks. Emerging architectures now integrate features such as signal reception and processing units, sensors, amplification units, and transmissive capabilities, along with sophisticated 3D structures.

These enhancements enable versatile operating modes, allowing RISs to improve network coverage in challenging environments and support innovative communication paradigms like next-generation multiple access, Integrated Sensing and Communications (ISAC), and energy harvesting. As such, RIS technology is set to transform the way we connect and communicate in the upcoming era of 6G, fundamentally altering the landscape of wireless networking.

2.2 High-Frequency Communication with RISs

Reconfigurable Intelligent Surfaces (RIS) demonstrate considerable potential as auxiliary devices in enhancing spectral efficiency, mitigating interference, and improving physical

security, among other benefits [23]. Notably, since RIS only passively reflects incoming signals, they operate in an energy-efficient manner, eliminating the need for radio frequency (RF) chains and thereby reducing energy consumption by orders of magnitude compared to traditional active antenna arrays. Additionally, due to their passive characteristics, RIS are free from self-interference and antenna noise amplification. Recent theoretical analyses indicate that RIS-assisted systems can achieve a quadratic scaling law in the received signal power, which scales quadratically with the number of passive units [23, 35]. These advantageous features position RIS as an appealing solution for overcoming signal blockage and improving coverage in millimeter-wave (mmWave) communications.

Channel state information (CSI) acquisition is essential for realizing the full potential of RIS-assisted mmWave systems. However, obtaining complete CSI for both the base station (BS)-RIS (B-R) link and the RIS-user (R-U) link is particularly challenging, as RIS cannot transmit or receive signals and lacks inherent signal processing capabilities. Moreover, acquiring the CSI typically requires substantial training overhead due to the extensive size of antenna arrays at the transceiver and the large number of passive elements at the RIS. Some recent efforts have sought to exploit the inherent sparse nature of the cascade BS-RIS-user mmWave channel, formulating the channel estimation problem within a compressed sensing (CS) framework. However, CS-based methods are often expensive to implement due to their excessive computational complexity.

On the other hand, many channel measurements [1] have indicated that mmWave channels exhibit sparse scattering characteristics. Notably, the power of the line-of-sight (LoS) path is significantly higher—approximately 13 dB higher in mmWave bands and 20 dB higher in terahertz bands—than the cumulative power of non-line-of-sight (NLoS) paths. Therefore, rather than obtaining the full CSI, an alternative strategy is to identify only the dominant path and align the transmitter's and receiver's beams to achieve sufficient beamforming gain for mmWave communications. This process, aimed at identifying one or several dominant paths for initial access, is commonly referred to as beam training (BT) or beam alignment (BA). In the context of RIS-assisted mmWave systems, BT seeks to simultaneously identify the optimal BA for both the B-R link and the R-U link. Given that RIS is a passive device that cannot transmit or receive signals, BT for RIS-assisted mmWave systems presents greater challenges compared to conventional mmWave systems.

2.3 Beam Training in RIS-Assisted Communication Systems

To effectively align the beams in this three-node communication system, BT involves estimating the angle of departure (AoD) and the angle of arrival (AoA) related to the dominant path of the B-R link, as well as the AoD and AoA associated with the dominant path of the R-U link. Given the cascade nature of the channel, RIS can form a reflecting beam by carefully devising its phase shift vector, which points in a direction that is a superposition of the incident angle and a "relative reflection" angle. This carefully devised phase shift vector resembles conventional steering vectors and can be characterized by the relative reflection angle (RRA). Thus, rather than searching for the AoA and AoD at the RIS, our objective is to identify the optimal RRA at the RIS to achieve BA for both the B-R and R-U links, significantly reducing the search space.

In practice, with knowledge of the BS location, RIS can be installed within the line of sight of the BS. Some existing studies [40] assume that the BS has aligned its beam to the RIS and focus on BT between the RIS and the user, which can be accomplished using conventional

BT techniques. However, this assumption is only valid for stationary BSs and RISs. With the rising popularity of unmanned aerial vehicles (UAVs) and their potential in wireless communications, mobile BSs based on UAVs are being considered for deployment in the near future. In such scenarios, it is essential to simultaneously identify the optimal BA for both the B-R link and the R-U link. Moreover, in practice, the LoS path between the BS and the RIS may be obstructed by obstacles, necessitating joint BS-RIS-user BT to find an alternative path from the BS to the user.

2.3.1 Exhaustive Search

An intuitive approach for beam training (BT) involves exhaustively searching all potential beam tuples or triplets. Specifically, the base station (BS), reconfigurable intelligent surface (RIS) and user, each utilize pre-defined codebooks, denoted as F_B, F_R, and F_U, respectively. These codebooks consist of a set of narrow beams, designed by uniformly quantizing the corresponding beam angles—namely, the angle of departure (AoD) for the BS and user, and the reflection angle (RRA) for the RIS. The finely quantized angles are assumed to uniformly cover the full range of AoD, AoA, and RRA angles. The optimal beam tuple for beam alignment (BA) is identified by exhaustively evaluating all possible combinations of $|F_B|$, $|F_R|$, and $|F_U|$ based on the received signal power.

This exhaustive search process requires the RIS to scan its entire RRA angular space for every beam direction chosen at the BS, while simultaneously the user must scan its entire AoA space for each combination of AoD and RRA. The use of pencil beams provides a significant advantage to this exhaustive search strategy, as the alignment of the beam tuple with the dominant path can yield substantial beamforming gains, facilitating the identification of the best BA even in low signal-to-noise ratio (SNR) environments. However, this straightforward approach incurs a prohibitively large training overhead. Assuming the BS has N_t antennas, the user has N_r antennas, and the RIS consists of a planar surface with $M = M_y \times M_z$ reflecting elements, achieving optimal spatial resolution requires the BS and user to utilize N_t and N_r narrow beams to thoroughly scan the AoA and AoD spaces, respectively, while the RIS must deploy M reflecting beams to explore the RRA domain. Consequently, the total number of beam tuples to be examined can reach up to $N_t N_r M$, leading to excessive delays during initial access [37].

2.3.2 Hierarchical Search

To accelerate the BA process, hierarchical multi-resolution beam search methods have been proposed for conventional mmWave systems. These hierarchical search techniques can be readily adapted for RIS-assisted systems, where the BS, RIS, and user each utilize their own multi-layer beamforming codebooks for joint spatial scanning. In this context, the lower-layer codebook employs wider beams compared to the higher-layer codebooks, with spatial resolution improving as the number of layers increases.

The hierarchical search process consists of multiple stages. At each stage, the respective layer's codebooks or subcodebooks are used for spatial scanning. This scanning method is similar to that of the exhaustive search, but focuses only on the range identified in the previous stage. The user assesses the received signal power to determine the best beam tuple, and this information is relayed back to the BS and RIS to adaptively select higher-resolution subcodebooks for subsequent stages of scanning. This iterative process continues until the desired spatial resolution is achieved.

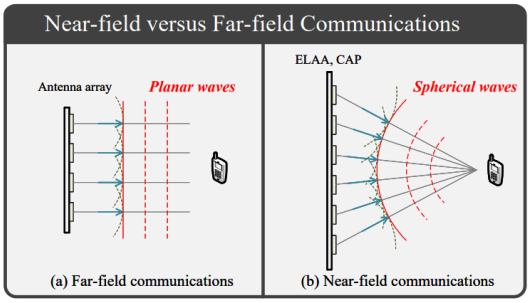

Figure 2.1: Comparison of near-field and far-field characteristics, adapted from [21]. The electromagnetic (EM) field radiated from antennas can be divided into two distinct regions: the near-field and far-field regions. In the far-field region, the wavefront of EM waves can be approximated as planar. Conversely, in the near-field region, more complex wavefront models, such as spherical waves, are required to accurately represent propagation characteristics.

Despite the considerable reduction in training overhead, a major drawback of hierarchical beam search is that the utilization of wider beams during earlier stages can lead to lower beamforming gains. Consequently, spatial scanning at lower levels may fail to detect the correct beam tuple in low SNR scenarios, potentially overlooking the dominant path. This challenge is exacerbated in RIS-assisted mmWave systems due to the significant product-path loss of the cascading channels. Furthermore, the hierarchical beam search approach requires frequent feedback from the user to the BS and RIS, adding extra demands to the training process. Lastly, because this method necessitates the BS and RIS to interact individually with each user, extending it to multi-user scenarios requires careful global coordination, posing another challenge for such systems.

2.3.3 RIS Phase Profile Codebooks

In this study, we aim to replicate and evaluate the novel variable-width hierarchical phase-shift codebook proposed in [4], which is applicable to both near- and far-field scenarios of Reconfigurable Intelligent Surfaces (RIS). This work emphasizes the significance of wireless communications within the radiating near-field region, employing a specific near-field channel model for beam management, as the curvature of wavefronts notably impacts communication performance at distances shorter than d_{FF}. The reactive near-field is typically constrained, with evanescent waves diminishing rapidly, underscoring the relevance of the radiating near-field in enhancing beam management strategies in modern communication systems.

To address these challenges, this study introduces a novel beam management framework for RIS-enabled mmWave multi-antenna communication systems, building on the wide illumination approach designed for low-overhead channel estimation (CE) in mobile scenarios. Furthermore, as illustrated in Figure 2.1, we can observe the distinct characteristics of the near-field and far-field regions, where the electromagnetic (EM) field radiated from antennas behaves differently. The figure highlights that, in the far-field region, the wavefront of EM waves can be approximated as planar, whereas in the near-field region, more complex wavefront models, such as spherical waves, are required to accurately represent propagation characteristics. Additionally, we examine the accompanying efficient alignment algorithm designed to optimize the phase shifts of the RIS and the beamformers of the transceiver. By conducting comprehensive performance evaluations, we assess the effectiveness of the proposed algorithm in [4] in relation to various benchmark schemes, thus highlighting its potential advantages and practical applicability in real-world scenarios.

3. BEAM MANAGEMENT FOR RIS-ASSISTED COMMUNICATION SYSTEMS

3.1 System and Channel Models

3.1.1 System Model

The communication system includes a base station (BS) with N_{bs} antennas, a reconfigurable intelligent surface (RIS) composed of $Q \triangleq Q_y Q_z$ tunable unit cells, with inter-element spacings d_y and d_z on the y- and z-axis, respectively (as discussed in [4]). The RIS unit cells are indexed by $q_y = 0, 1, \ldots, Q_y - 1$ and $q_z = 0, 1, \ldots, Q_z - 1$. Additionally, there is a mobile user (MU) with N_{mu} antennas. In the downlink direction, the baseband signal received at the MU antennas, $\boldsymbol{y}_{\text{mu}} \in \mathbb{C}^{N_{\text{mu}} \times 1}$, can be expressed as:

$$\boldsymbol{y}_{\text{mu}} = (\boldsymbol{H} + \boldsymbol{H}_2 \boldsymbol{\Omega} \boldsymbol{H}_1)\, \boldsymbol{x}_{\text{bs}} + \boldsymbol{n}_{\text{mu}}, \tag{3.1}$$

where $\boldsymbol{x}_{\text{bs}} \in \mathbb{C}^{N_{\text{bs}} \times 1}$ is the signal transmitted by the BS. The transmitted signal power satisfies $\mathbb{E}\left\{\|\boldsymbol{x}_{\text{bs}}\|^2\right\} \leq P_{\text{bs}}$, where P_{bs} is the total transmit power, and $\boldsymbol{n}_{\text{mu}} \sim \mathcal{CN}(0, \sigma^2_{\text{mu}} \boldsymbol{I}_{N_{\text{mu}}})$ represents the additive white Gaussian noise (AWGN) at the MU receiver.

The $Q \times Q$ diagonal matrix $\boldsymbol{\Omega}$ in (3.1) is defined as:

$$\boldsymbol{\Omega} \triangleq \text{diag}\left(\left[g e^{j\omega_1}, g e^{j\omega_2}, \ldots, g e^{j\omega_Q}\right]\right), \tag{3.2}$$

where each ω_q (with $q = 1, 2, \ldots, Q$) is the phase shift applied by the q-th RIS unit cell and $g \triangleq \frac{4\pi d_y d_z}{\lambda^2}$ is a dimensionless factor that depends on the wavelength λ and the inter-element spacings d_y and d_z.

Additionally, $\boldsymbol{H} \in \mathbb{C}^{N_{\text{mu}} \times N_{\text{bs}}}$, $\boldsymbol{H}_1 \in \mathbb{C}^{Q \times N_{\text{bs}}}$, and $\boldsymbol{H}_2 \in \mathbb{C}^{N_{\text{mu}} \times Q}$ represent the channel matrices for the BS-MU, BS-RIS, and RIS-MU links, respectively.

It is assumed the MU is capable of fully digital combining of the received signal $\boldsymbol{y}_{\text{mu}}$ using a vector $\boldsymbol{u}_{\text{mu}} \in \mathbb{C}^{N_{\text{mu}}}$, and that $\|\boldsymbol{u}_{\text{mu}}\| = 1$.

3.1.2 Near-Field Channel Model

To distinguish between far-field and near-field conditions, we use the critical distance, beyond which the phase error from assuming a planar wavefront in the far-field is no more than $\pi/8$. This distance is defined as $d_F \triangleq \frac{2D^2}{\lambda}$, where D is the largest dimension of the RIS in meters.

As shown in Figure 3.1, the critical distance d_F exhibits different behaviors based on the physical size of the Reconfigurable Intelligent Surface (RIS) and the number of unit cells Q. When the physical size L is held constant, the critical distance d_F increases with frequency due to the reduction in wavelength λ, allowing the RIS to more effectively manipulate the incident waves. In contrast, when the number of unit cells Q is constant, d_F decreases with frequency. This occurs because the spacing d between unit cells decreases as frequency increases, which diminishes the RIS's ability to extend its influence over longer distances. Thus, the relationship between critical distance, frequency, and the physical configuration of the RIS is pivotal in optimizing its performance in wireless communication systems.

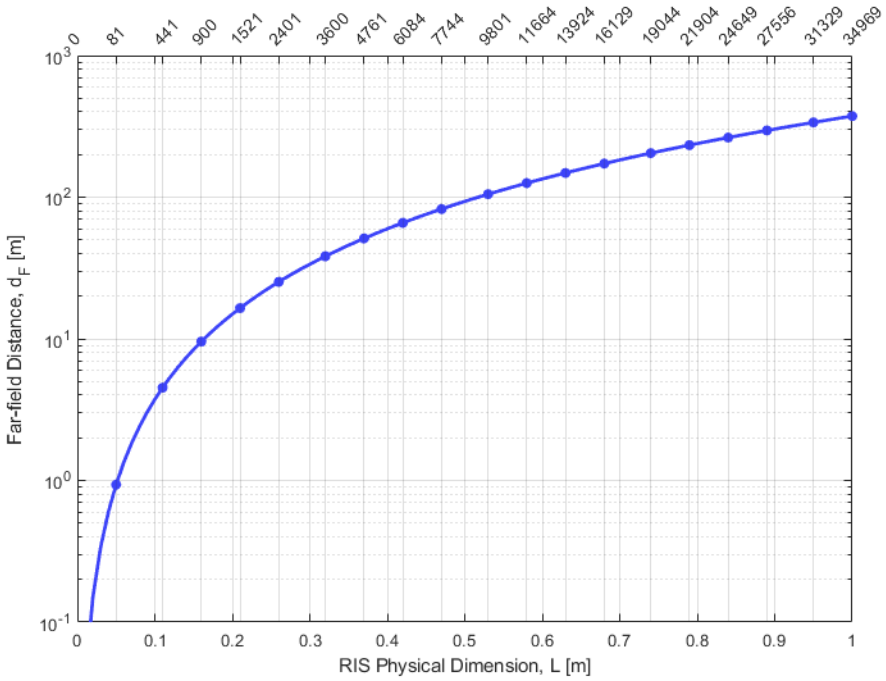

Figure 3.1: Far-field distance versus the RIS physical dimension $L_y = L_z \triangleq L$ (i.e., $D = \sqrt{L_y^2 + L_z^2} = \sqrt{2}L$) and the number of its unit elements Q for 28 GHz carrier frequency and element spacing $d_y = d_z \triangleq d = \lambda/2$.

The wireless channels are modeled as a collection of propagation paths. For the BS-RIS link with ℓ_1 paths, the channel gain between the m-th BS antenna (with $m = 1, 2, \ldots, N_{\text{bs}}$) and the q-th RIS element, where the distance in the i-th path is $d_{1,i,qm}$, is expressed as:

$$[\boldsymbol{H}_1]_{q,m} \triangleq \sum_{i=0}^{\ell_1 - 1} \text{PL}_{1,i} \gamma_{1,i} e^{\jmath \frac{2\pi}{\lambda} d_{1,i,qm}}, \tag{3.3}$$

where $\text{PL}_{1,i}$ and $\gamma_{1,i}$ represent the path loss and small-scale fading of the BS-RIS link, respectively.

Similarly, the BS-MU and RIS-MU channel matrix elements are given by:

$$[\boldsymbol{H}]_{n,m} \triangleq \sum_{i=0}^{\ell_h - 1} \text{PL}_{h,i} \gamma_{h,i} e^{\jmath \frac{2\pi}{\lambda} d_{h,i,nm}}, \tag{3.4}$$

and

$$[\boldsymbol{H}_2]_{n,q} \triangleq \sum_{i=0}^{\ell_2 - 1} \text{PL}_{2,i} \gamma_{2,i} e^{\jmath \frac{2\pi}{\lambda} d_{2,i,nq}}, \tag{3.5}$$

where $\text{PL}_{h,i}$ and $\gamma_{h,i}$ represent the path loss and small-scale fading of the BS-MU link and $\text{PL}_{2,i}$ and $\gamma_{2,i}$ represent the path loss and small-scale fading of the RIS-MU link. The tests are focused on scenarios where the BS-RIS and RIS-MU links have a dominant line-of-sight (LOS) component (with index $i = 0$) and their distances are less than d_F.

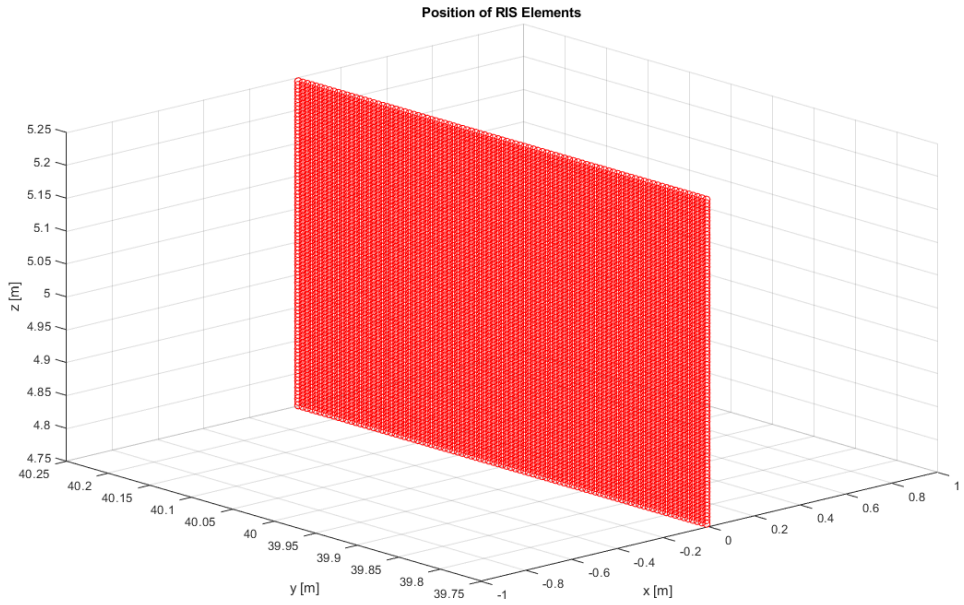

Figure 3.2: Visualization of the spatial distribution and arrangement of reflective elements on the RIS used for optimizing signal reflections in the communication environment.

3.1.3 The Ricean Factor

To account for both line-of-sight (LOS) and non-line-of-sight (NLOS) components in the channel, we employ the Ricean factor K, which defines the relative power between the LOS and NLOS components. This model is particularly relevant in millimeter-wave (mmWave) communication systems, where the LOS path often dominates signal propagation. For our analysis, the performance of various algorithms is compared against benchmark schemes using the Ricean fading model, where N_t and N_r denote the number of transmitting and receiving antennas, respectively.

The Ricean fading channel model with K factor is represented by:

$$\mathsf{H} = \sqrt{\frac{K}{1+K}}\mathsf{H}_{\text{LOS}} + \sqrt{\frac{1}{1+K}}\mathsf{H}_{w},$$

where H_{LOS} represents the deterministic LOS component, H_w represents the NLOS scattering component, and K is the Rice factor. The channel matrix H has dimensions $N_r \times N_t$, where each element models the channel response between a transmitting antenna and a receiving antenna. For the channel matrix H to be normalized, $\|\mathsf{H}_{\text{LOS}}\|_F^2 = N_t N_r$.

3.2 Beam Management Framework

In this section, we analyze the design of a set of hierarchical RIS phase-shift codebooks, denoted as $\mathcal{W}_1, \mathcal{W}_2, \ldots, \mathcal{W}_W$, where $|\mathcal{W}_1| < |\mathcal{W}_2| < \cdots < |\mathcal{W}_W|$. Each codebook $\mathcal{W}_w$ contains $|\mathcal{W}_w|$ phase-shift configurations, $\omega_{w,k_w} = [\omega_{w,k_w,1}, \ldots, \omega_{w,k_w,Q}]$, for $w = 1, 2, \ldots, W$ and $k_w = 1, 2, \ldots, |\mathcal{W}_w|$. The near-field phase-shift design from [16] is used to create these codebooks.

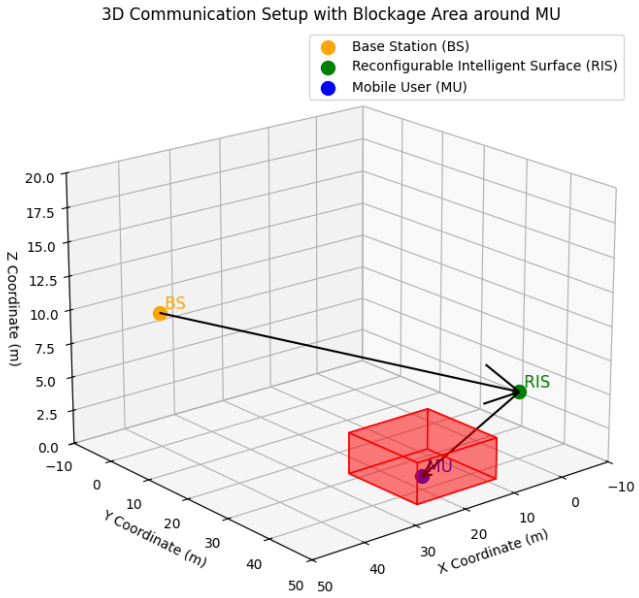

Figure 3.3: The red rectangular prism represents the blockage area surrounding the BS, simulating the impact of physical obstructions on signal propagation. The arrows indicate line-of-sight (LOS) paths between the BS, RIS, and MU.

3.2.1 Near-Field Hierarchical Codebook Design

Treating the BS and the MU as point source, leads to the following expression for RIS's realized gain in the near-field g_{RIS}:

$$g_{\text{RIS}}(\mathbf{p}_i, \mathbf{p}_r) \triangleq g \sum_{n=0}^{Q-1} e^{j\frac{2\pi}{\lambda}(\|\mathbf{p}_i - \mathbf{p}_n\| + \|\mathbf{p}_r - \mathbf{p}_n\|)} e^{j\omega_n}, \tag{3.6}$$

where $\mathbf{p}_i$, $\mathbf{p}_r$, and $\mathbf{p}_n$ represent the positions of the BS, the observation point, and the n-th RIS element, respectively.

Focusing on the LOS paths between the BS, RIS, and MU and assuming the blockage area is rectangular, centered at $\mathbf{p}_b$ with length R_x and width R_y, it is defined as $\mathbf{p}_r \in \mathcal{P}_r = \{\mathbf{p} = \mathbf{p}_b + [x, y, 0] : x \in [-R_x/2, R_x/2], y \in [-R_y/2, R_y/2]\}$.

The RIS phase-shift profile is:

$$\omega_n = -\frac{2\pi}{\lambda} \left(\|M(\mathbf{p}_n) - \mathbf{p}_n\| - \|M(\mathbf{p}_n) - \mathbf{p}_{\text{RIS}}\| + \|\mathbf{p}_i - \mathbf{p}_n\| \right), \forall n, \tag{3.7}$$

where $\mathbf{p}_{\text{RIS}}$ is the RIS center, and $M(\mathbf{p}_n)$ maps $\mathbf{p}_n$ to a point in the blockage area $\mathbf{p}_r \in \mathcal{P}_r$ as:

$$M(\mathbf{p}_n) = \mathbf{p}_r + \left(\frac{\Delta_x}{L_z} z + x w_x, \frac{\Delta_y}{L_y} y + y w_y, 0 \right), \tag{3.8}$$

where $w_t = \frac{w_t R_t}{W_t} - R_t/2$ and $\Delta_t = \frac{\alpha R_t}{W_t}$, with $w_t = 0, 1, \ldots, W_t - 1$ and $t \in \{x, y\}$.

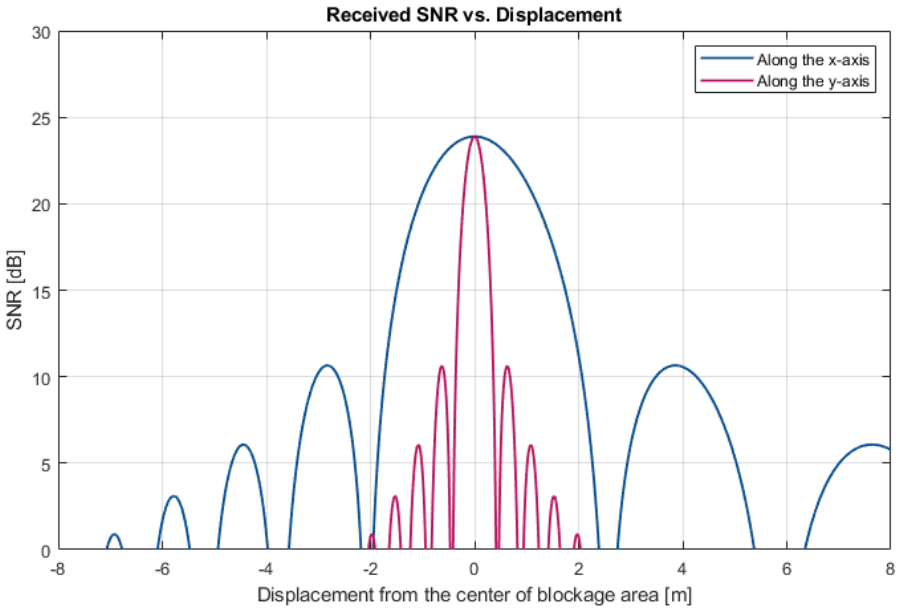

Figure 3.4: Received SNR vs. the displacement along the x- and y-axes when the RIS is configured to focus on the center of the blockage area. BS is at $\mathbf{p}_i = [40, 0, 10]$ and RIS is at $\mathbf{p}_{\text{ris}} = [0, 40, 5]$, the focus point is at $\mathbf{p}_b = [20, 40, 1]$; $L_y = L_z = 0.5m$; $d_y = d_z = \frac{\lambda}{2}$; and $f = 28$ GHz.

For narrow illumination, the values W_x and W_y can differ due to beam spread differences. Focusing the RIS on $\mathbf{p}_b$, we get the phase-shift profile:

$$\omega_n = \sum_{t\in\{y,z\}} -\frac{2\pi d_t}{\lambda} \left(\|\mathbf{p}_i - \mathbf{p}_n\| + \|\mathbf{p}_b - \mathbf{p}_n\|\right), \forall n. \tag{3.9}$$

This achieves the maximum $g_{\text{max}} = gQ$ at point $\mathbf{p}_b$.

In Figure 3.4, we plot the SNR of the RIS-enabled link as:

$$\text{SNR} \triangleq \frac{P_{\text{BS}} \left|g_{\text{RIS}}(\mathbf{p}_i, \mathbf{p}_r)\right|^2}{\sigma^2_{\text{MU}}} \cdot PL(p_i, p_r), \tag{3.10}$$

where $PL(\mathbf{p}_i, \mathbf{p}_r)$ represents the cascaded path loss between the $\mathbf{p}_i$ and the $\mathbf{p}_r$ based on displacements δ_x and δ_y from $\mathbf{p}_b$.

As shown in Figure 3.4, the plot highlights that the power distributions along the two axes exhibit significantly different behaviors due to the way the RIS focuses the beams and how the waves propagate in space.

The y-axis exhibits a narrow, regular beam spread, with a sharp drop in SNR as displacement increases. This indicates a more focused energy concentration along the y-direction, where precise alignment is required for optimal reception.

Along the x-axis, the beam widens as displacement increases, resulting in a more gradual SNR decay and a larger coverage area. This is due to wave propagation along the x-axis, which causes the beam to spread further.

Periodic side lobes appear along both axes due to constructive and destructive interference from the RIS, more pronounced in the x-direction due to the wider beam spread.

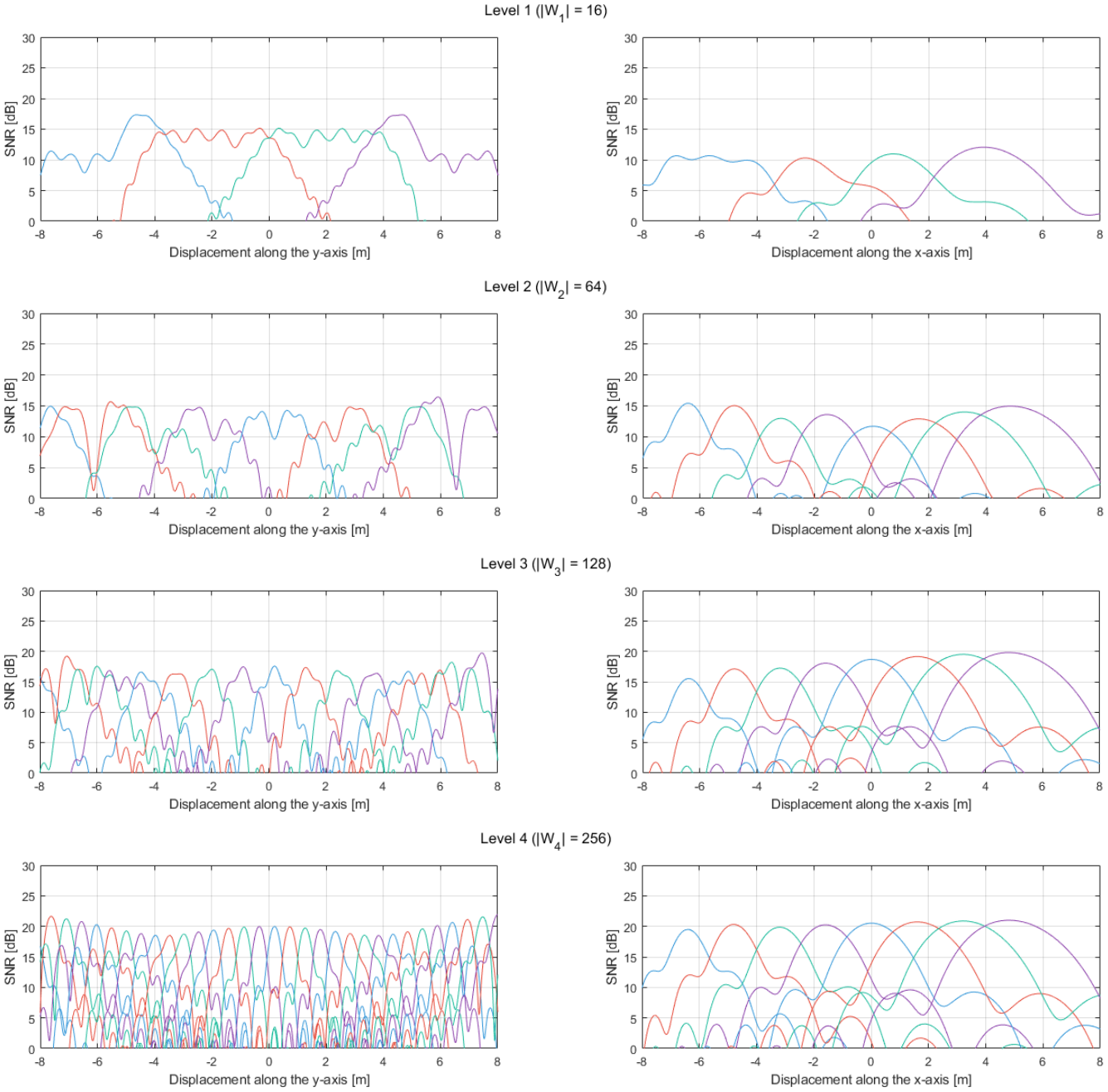

Figure 3.5: Four-level hierarchical RIS phase-shift codebook for near-field illumination constructed from (5) with $\alpha = 0.8$. The x- and y-axes of the blockage area are divided into $W_x = 4$ and $W_y = 4$ sub-areas for Level 1, $W_x = 8$ and $W_y = 8$ sub-areas for Level 2, $W_x = 8$ and $W_y = 16$ sub-areas for Level 3, and $W_x = 8$ and $W_y = 32$ sub-areas for Level 4.

Given the system setup, the beam along the x-axis spreads more as distance increases. For narrow illumination, W_y should be chosen larger than W_x to adequately cover the blockage area, since the beam along the y-axis remains more confined while the x-axis beam spreads wider.

Figure 3.5 presents a multi-level codebook design, adapted from [4], illustrating a structured approach with $W = 4$ distinct levels. Each level is characterized by its unique size, specifically $(W_x, W_y) = (4, 4), (8, 8), (8, 16), (8, 32)$. This hierarchical structure allows for a systematic exploration of the beamforming capabilities of the reconfigurable intelligent surface (RIS).

At the initial levels, the codebook is relatively smaller, which facilitates a faster selection process. As we progress to the higher levels, the sizes increase, thereby offering a greater variety of beam patterns to choose from. This escalation in complexity is crucial for fine-tuning the phase shifts and optimizing the beam alignment with the mobile user (MU).

Notably, a RIS configuration with $Q = 8649$, reflecting a substantial number of elements, and $W = 256$, representing an extensive codebook size, achieves a peak Signal-to-Noise Ratio (SNR) of 22 dB. This level of SNR indicates effective beam management and phase-shift optimization, significantly enhancing overall communication performance. The ability to attain such a high peak SNR underscores the potential of utilizing multi-level codebooks in RIS-assisted systems, enabling more robust connections and improved signal quality for users.

3.2.2 RIS Phase-Shift Management

In this section, we discuss the design of RIS phase-shift profiles while employing base station (BS) precoding and mobile user (MU) combining designs. The RIS is positioned to maintain a strong line-of-sight (LOS) connection with both the BS and the MU. Given that both the BS and RIS are fixed, we consider a static precoder, $\mathbf{v}_{\mathsf{bs}}$, which is optimized to focus on the center of the RIS.

However, since the MU may not be aware of the RIS's exact location, it utilizes a set of combiners, denoted as $\mathcal{W}_{\mathsf{mu}}$, selecting the one that maximizes the received signal power. The RIS phase-shift profile, represented as $\Omega_{w,k_w} = g\,\mathsf{diag}(e^{j\omega_{w,k_w}})$, corresponds to the k_w-th codeword from the w-th level codebook $\mathcal{W}_w$.

The instantaneous signal-to-noise ratio (SNR) at the MU is given by:

$$\mathsf{SNR}_{\mathsf{mu}}(\Omega_{w,k_w}) = \max_{\mathbf{u}_{\mathsf{mu}} \in \mathcal{W}_{\mathsf{mu}}} \frac{\|\mathbf{u}_{\mathsf{mu}}^H \left(\mathbf{H} + \mathbf{H}_2 \Omega_{w,k_w} \mathbf{H}_1\right) \mathbf{v}_{\mathsf{bs}}\|^2}{\sigma_{\mathsf{mu}}^2}, \tag{3.11}$$

where $\|\mathbf{u}_{\mathsf{mu}}\| = 1$ for all $\mathbf{u}_{\mathsf{mu}} \in \mathcal{W}_{\mathsf{mu}}$.

During each SNR measurement, the BS transmits pilot symbols, the RIS selects a phase-shift configuration Ω_{w,k_w}, and the MU computes $\mathsf{SNR}_{\mathsf{mu}}(\Omega_{w,k_w})$. Subsequently, for each level of the RIS codebook, the MU reports the index of the phase shift that yields the maximum SNR back to the RIS controller via a feedback link. This is mathematically represented as:

$$k_w^* = \arg \max_{k_w \in K_w^*} \mathsf{SNR}_{\mathsf{mu}}(\Omega_{w,k_w}), \tag{3.12}$$

where $K_w^* \subset \{1, 2, \ldots, |\mathcal{W}_w|\}$ is the subset of phase-shift indices used at the w-th codebook level. Notably, the first level of the codebook is not reduced, i.e., $K_1^* \triangleq \{1, 2, \ldots, |\mathcal{W}_1|\}$. The selection of k_w^* by the RIS helps define K_{w+1}^*, thereby narrowing down the search in the subsequent codebook level.

The hierarchical RIS beam management approach is summarized in the algorithm below, focusing on the selection of the optimal beams that trace the best "path" within the codebook hierarchy. This approach is designed to identify the beam configuration that maximizes the estimated SNR, progressively refining the search space based on previously returned top-performing beams.

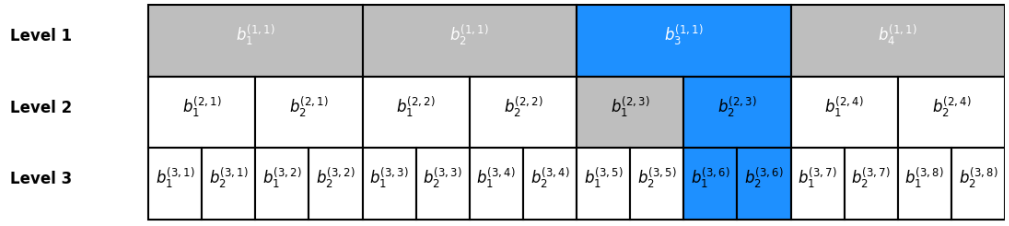

Figure 3.6: The gray marked fields represent the beams that have been tested, but did not lead to a high received SNR. The blue fields represent the beams that have been tested and lead to a high received SNR. In Level 1 we had to test all four possible beams. In Level 2, we could focus on the beams that correspond to $b_3^{(1,1)}$, because this beam lead to the highest SNR, namely $b_1^{(2,3)}$ and $b_2^{(2,3)}$. In Level 3, we had to test $b_1^{(3,6)}$ and $b_2^{(3,6)}$. In the end, we found the beam $b_1^{(3,6)}$, that leads to the best result, just as if we would have tested all entries of Level 3.

Hierarchical RIS Beam Management

Input: Codebook sets for each level $\mathcal{W}_1, \mathcal{W}_2, \ldots, \mathcal{W}_W$
Output: Best beam indices for each level $k_1^*, k_2^*, \ldots, k_W^*$
for $w = 1$ to W **do**
  if $w == 1$ **then**
    $\mathcal{K}_w \leftarrow \{1, 2, \ldots, |\mathcal{W}_w|\}$
  else
    $\mathcal{K}_w \leftarrow$ Beams corresponding to best beam k_{w-1}^*
  end if
  $\text{SNR}_{\text{best}} \leftarrow -\infty$
  $k_w^* \leftarrow 0$
  for each $k_w \in \mathcal{K}_w$ **do**
    Set phase shift: Ω_{w,k_w}
    Compute SNR: $\text{SNR}_{\text{mu}}(\Omega_{w,k_w})$
    if $\text{SNR}_{\text{mu}}(\Omega_{w,k_w}) > \text{SNR}_{\text{best}}$ **then**
      $\text{SNR}_{\text{best}} \leftarrow \text{SNR}_{\text{mu}}(\Omega_{w,k_w})$
      $k_w^* \leftarrow k_w$
    end if
  end for
  Store best beam index k_w^* for level w
end for
Return: Optimal beam indices $k_1^*, k_2^*, \ldots, k_W^*$

To further illustrate the beam management process, consider a naive approach that would involve evaluating every possible beam across all levels of the codebook without any prior selection criteria. In this approach, the algorithm would compute the Signal-to-Noise Ratio (SNR) for each beam independently at every level, leading to an exhaustive search at each stage. This means that for the first level, all available beams would be tested, and the one with the highest SNR would be selected. As the algorithm progresses to subsequent levels, it would continue to test all beams, ignoring any prior knowledge about which beams performed well in earlier evaluations. While this method ensures a thorough exploration of all potential options, it incurs significant computational overhead and may require extensive time and resources to complete the beam selection process. In contrast, the hierarchical method intelligently narrows down the candidate beams based on prior results, thereby enhancing efficiency while still aiming for optimal performance.

4. NUMERICAL RESULTS AND DISCUSSION

In this chapter, we explore the performance of different beam management strategies within a Ricean fading environment. Specifically, we will first evaluate a naive hierarchical search approach that examines every beam across all levels of the codebook, regardless of prior knowledge. This exhaustive method will serve as a baseline against which we will compare the proposed hierarchical search algorithm in [4], which intelligently narrows down candidate beams based on the results from prior levels, aiming to improve efficiency while optimizing performance.

4.1 Simulation Parameters and Setup

The simulation adopts the following parameters: a carrier frequency of $f = 28$ GHz and half-wavelength antenna element spacing at all nodes. The Base Station (BS) is equipped with one $N_{\text{bs}} = 1$ antenna, situated in the $x-z$ plane with its center at $\mathbf{p}_{\text{bs}} = [40, 0, 10]$. The Reconfigurable Intelligent Surface (RIS) consists of a square aperture measuring $L_y = L_z = 0.5$ m (i.e., $Q = 8649$), located in the $y-z$ plane with its center at $\mathbf{p}_{\text{ris}} = [0, 40, 5]$. Although the proposed algorithm in [4] can accommodate multi-antenna Mobile Users (MUs), we assume a single-antenna MU ($N_{\text{mu}} = 1$) to facilitate a straightforward comparison with the optimal case of full channel state information (CSI). Since we consider a Single Input Single Output (SISO) case in the results section, the channel matrices $\boldsymbol{H}_1$ in (3.3) and $\boldsymbol{H}_2$ in (3.5) reduce to vectors, which we denote as $\boldsymbol{h}_1 \in \mathbb{C}^{Q\times 1}$ and $\boldsymbol{h}_2 \in \mathbb{C}^{1\times Q}$, while $\boldsymbol{H}$ in (3.4) becomes a scalar quantity $h \in \mathbb{C}$.

The MU is placed within a square blockage area measuring $R_x \times R_y$, centered at $\mathbf{p}_{\text{mu}} = [20, 40, 1]$, with $R_x = R_y = 16$ m. The direct BS-MU link is characterized by a 20 dB attenuation factor. The propagation environment is modeled to include 1 non-line-of-sight (NLOS) scattering path for each link—BS-RIS, BS-MU, and RIS-MU—resulting in $\ell_1 = \ell_2 = \ell_h = 1$.

The BS transmits at $P_{\text{bs}} = 20$ dBm, with a noise spectral density of -176 dB/Hz, a bandwidth of $B = 100$ MHz, and a noise figure of $N_0 = 6$ dB. The simulation results are averaged over 200 random realizations of MU positions.

4.2 Benchmarks

The Hierarchical Algorithm in [4] employs a four-level hierarchical RIS phase-shift codebook, as illustrated in Figure 3.5. The naive method conducts an exhaustive search over the largest codebook (Level 4), which contains 256 phase-shift configurations, to identify the optimal solution. The hierarchical method intelligently narrows down candidate beams based on the results from prior levels, aiming to improve efficiency while optimizing performance.

For comparison, we consider also the following benchmarks:

- **Benchmark 1 (Full Focusing)**: In this scenario, the exact position of the MU is assumed to be perfectly known, allowing the RIS to adjust its phase shifts accordingly to focus on this specific position based on geometric information.

- **Benchmark 2 (Full CSI)**: This benchmark assumes perfect knowledge of the channels between the BS-RIS (h_1) and RIS-MU (h_2). The optimal RIS phase shifts are determined to maximize the end-to-end channel gain by aligning the phases of h_1 and h_2 such that $[\mathbf{\Omega}]_{q,q} = -[\angle h_1]_q - [\angle h_2]_q$ for all $q = 1, 2, 3, \ldots, Q$.
- **Benchmark 3 (Full Codebook Search)**: In this benchmark, we consider the largest codebook (i.e., Level 4 with 256 phase-shift configurations) and perform a full search across all possible configurations to find the optimal phase shifts that yield the highest received SNR at the MU.

4.3 Results

4.3.1 Naive Hierarchical Algorithm

To assess the performance of each level in the hierarchical codebook, we evaluated the SNR for each beam across all levels, selecting the beam with the highest SNR at each stage. This systematic selection process ensures that we capture the optimal beam alignment achievable at each level, allowing for a thorough comparison of performance across the hierarchy. The following figure presents the average received SNR across the different schemes. We assume free-space path loss for the LOS paths and change the relative power of non-LOS paths to vary Ricean factor K. It is noteworthy that in all cases, the SNR consistently improves as the Ricean factor increases. This trend is expected, as a higher Ricean factor signifies a stronger line-of-sight (LOS) component relative to the non-line-of-sight (NLOS) elements, which reduces signal scattering and interference from multipath components, thereby enhancing overall signal quality. The Ricean model's emphasis on the LOS component is particularly advantageous in structured environments, where it allows us to effectively harness the most stable propagation paths for improved SNR.

As anticipated, Benchmark 1 (Full CSI) delivers the highest performance due to complete channel state information, followed by Benchmark 2 (Full Focusing), and then Benchmark 3 (Full Codebook Search). For the Full Codebook Search, we tested all beams at each level, retaining the beam that yielded the highest SNR from the entire hierarchical codebook. Notably, we observe that the performance at Level 1 is comparatively limited, showing minimal improvement across varying values of the Ricean factor. Levels 2 and 3 exhibit similar performance potential, with slight differences. Meanwhile, Level 4 achieves results close to those of the Full Codebook Search, as it is the most refined level in the hierarchy, providing more granular beamforming control.

These observations confirm the effectiveness of hierarchical beam alignment in improving SNR, with higher levels offering increasingly targeted beam control that approaches the optimal performance of Full Codebook Search.

4.3.2 The Hierarchical Algorithm of [4]

We next evaluate the performance of the novel framework proposed in [4], designed to achieve results with even lower overhead. As anticipated, for nearly all values of the Ricean factor K_h, the schemes can be ranked in descending order of performance as: Benchmark 1, Benchmark 2, Benchmark 3, and the Hierarchical Algorithm of [4].

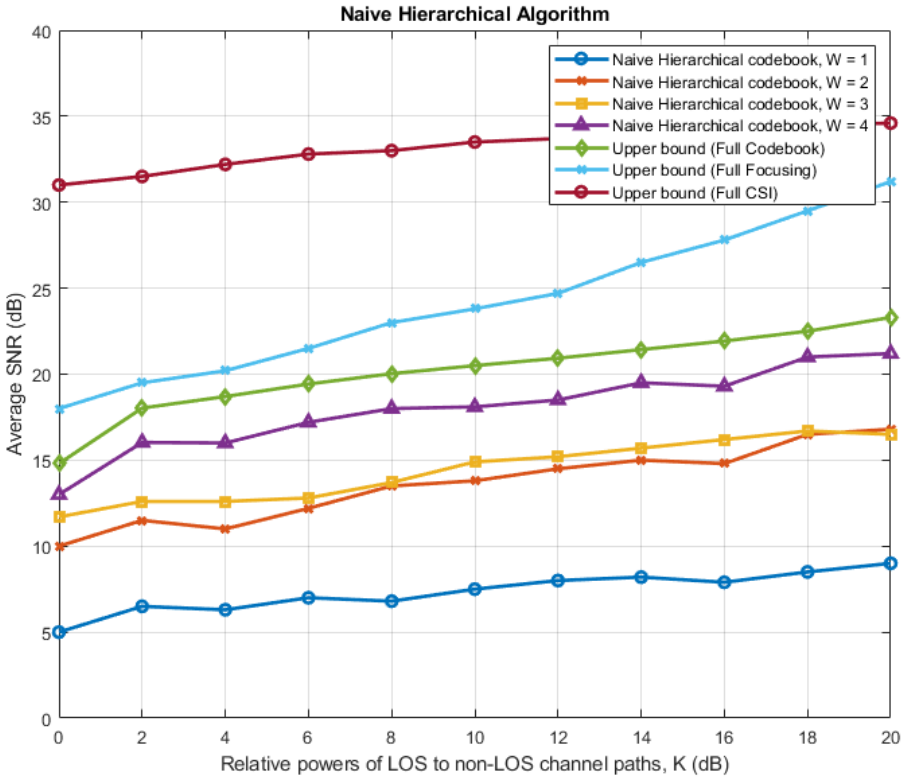

Figure 4.1: Naive Hierarchical Algorithm: Average received SNR at the MU (dB) vs. the relative powers of the LOS path with respect to the non-LOS paths (dB).

Specifically, Benchmark 1 achieves the highest performance when non-LOS (NLOS) paths are dominant—a scenario generally uncommon in mmWave communication systems [4].

In LOS-dominated scenarios, however, the performance of Benchmark 1 closely aligns with that of the remaining schemes, which are tailored to leverage the LOS path. Notably, the performance of all schemes, except for Benchmark 1, remains relatively consistent across the entire range of K_h values. This stability can be attributed to the narrow transmission beams characteristic of mmWave frequencies, which imply that, despite the presence of multiple channel scatterers, only a few will likely intersect the transmission beams.

Overall, the performance results of the Hierarchical Algorithm of [4] closely resemble those obtained through a naive full codebook search. The key distinction, however, lies in the efficiency of the algorithm: this novel framework iterates through the hierarchical codebook across all levels, achieving performance that is comparable to a Full Codebook Search while significantly reducing computational overhead. Consequently, the Hierarchical Algorithm of [4] offers a resource-efficient approach to beam alignment in mmWave systems, striking a commendable balance between performance and overhead. This makes it particularly well-suited for practical applications in RIS-enabled mmWave communication systems.

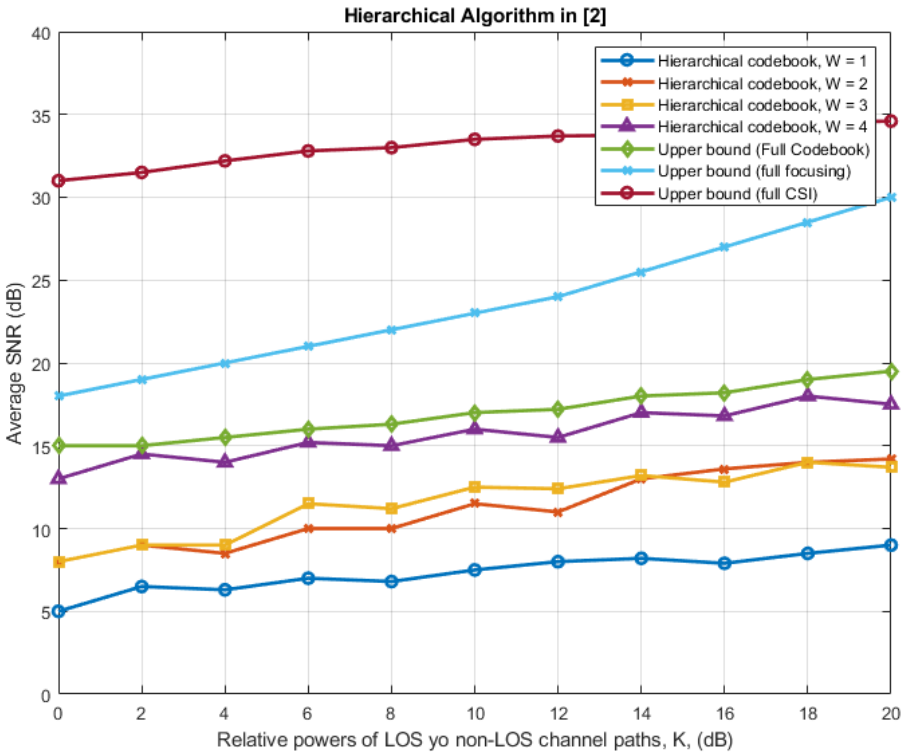

Figure 4.2: Hierarchical Algorithm in [4]: Average received SNR at the MU (dB) vs. the relative powers of the LOS path with respect to the non-LOS paths (dB).

4.4 Performance Comparison

The Table 4.1 provides a structured comparison of the methods based on critical attributes—SNR, channel knowledge, overhead, and complexity. Each approach is evaluated for its strengths and weaknesses relative to performance and resource requirements:

- **Hierarchical Approach:** While it yields a high SNR, this method is particularly advantageous in terms of reduced channel knowledge requirements and lower overhead. Its moderate complexity strikes a balance between performance and resource efficiency, making it a practical choice for applications with limited computational resources or communication overhead constraints.
- **Full CSI Approach:** With very high SNR performance, this method leverages full channel knowledge, resulting in substantial overhead and high complexity. This makes it suitable primarily for scenarios where resources are abundant, and performance is a priority over efficiency.
- **Full Focusing Approach:** Although offering high SNR and requiring full channel knowledge, this approach balances better than Full CSI in terms of moderate overhead, which may be more feasible in mid-complexity scenarios. It is a viable alternative when some trade-off between overhead and performance can be accommodated.

Table 4.1: Comparison of Methods Based on SNR and Attributes.

Attributes	Hierarchical	Full CSI	Full Focusing
SNR (dB)	High	Very High	High
Channel Knowledge	Partial	Full	Full
Overhead	Low	High	Moderate
Complexity	Moderate	High	High
Use Case	Suitable for low-overhead scenarios	Ideal for high-performance applications	Balanced applications with moderate requirements

The table effectively highlights how each method aligns with different performance and resource considerations, serving as a quick reference for selecting the most appropriate beamforming strategy based on application requirements.

5. CONCLUSIONS AND FUTURE WORK

This thesis aimed to replicate and analyze key experiments from recent work on near-field beam management for RIS-enabled millimeter-wave multi-antenna systems. Through detailed simulations, the study not only validated the effectiveness of hierarchical phase-shift codebooks in optimizing beam alignment but also rigorously tested the Hierarchical Algorithm of [4] across a diverse range of antenna configurations and varying numbers of scattering paths. This comprehensive approach provided a more nuanced understanding of the algorithm's performance and its adaptability to different operational scenarios. The results confirmed that RIS technology can significantly improve signal coverage and energy efficiency, particularly in dense urban environments where near-field communication is prevalent. The simulations highlighted how RIS can mitigate the limitations of traditional multi-antenna systems by enhancing signal quality and reliability, thereby supporting higher data rates and improving user experience.

However, several limitations were identified during the experiments. While the complexity of the near-field beam management algorithms was notably reduced compared to traditional methods, challenges remain in their real-time application. Achieving precise beam alignment in highly dynamic environments—where user mobility and environmental conditions fluctuate—may require more sophisticated control mechanisms. Furthermore, the performance of the Hierarchical Algorithm of [4] may vary significantly with different antenna configurations, factors affecting their gain, and the number of scattering paths present in the environment. This variability necessitates further investigation and adaptation of the algorithm to ensure consistent performance across diverse real-world conditions.

Future research can explore several avenues to further enhance RIS-based beam management systems. First, improving the scalability of the hierarchical codebook to accommodate larger arrays of RIS elements and more complex network configurations would be an important step. The integration of scalable algorithms could allow for the deployment of RIS in extensive networks, thus maximizing the benefits of this technology. Second, positioning plays a crucial role in beam alignment, particularly in scenarios where RIS is deployed in dynamic environments with user mobility. As demonstrated in [2], efficient beam alignment can be achieved by leveraging position information from sensors attached to nodes, which enables rapid adjustments to beam direction following any declared misalignment. This positioning-based approach facilitates alignment within just two rounds of control information exchange, ensuring that communication ends can optimize beamforming (BF) with minimal overhead. For scenarios requiring reduced computational overhead, one could explore a strategy where only a certain SNR threshold needs to be achieved, subject to the user equipment's quality-of-service constraints. This approach could potentially terminate the algorithm at an upper layer without needing to search through all available beams to acquire the optimal one, thus balancing performance with resource efficiency.

Furthermore, machine learning techniques could be applied to predict optimal phase-shift configurations dynamically, reducing the need for extensive channel state information (CSI) acquisition and thereby expediting the beam alignment process. Recent discoveries in artificial neural networks (ANNs) show promise for handling hardware nonlinearities and managing wireless channel dynamics efficiently [3]. For instance, efficient ANN-based configurations can address nonlinearities in multiple power amplifiers, as explored in full-duplex (FD) massive MIMO architectures for high-frequency communications.

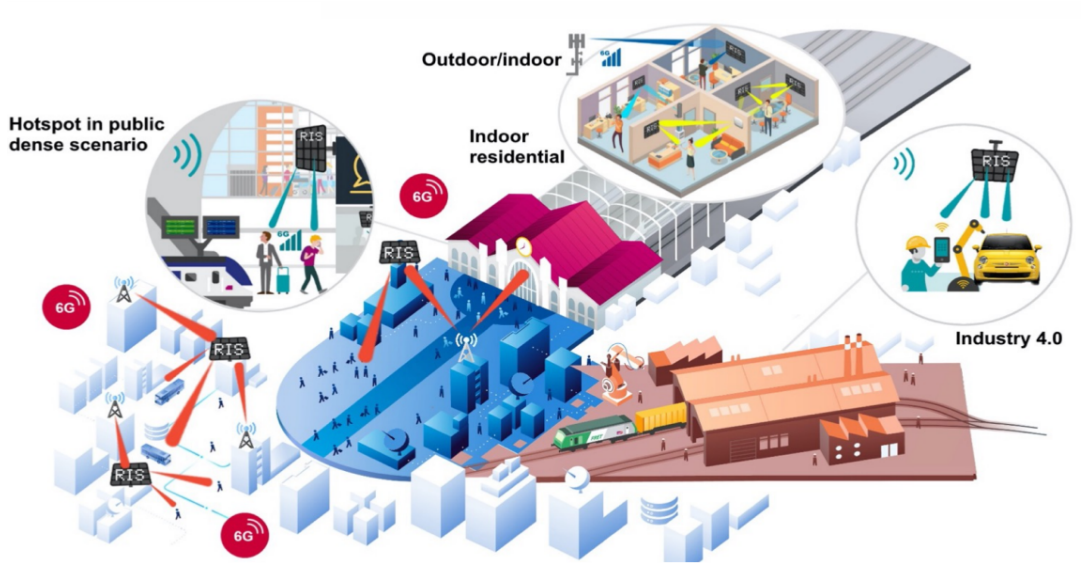

Figure 5.1: Applications of the proposed in [30] RISE wireless connectivity paradigm, enabled by a plurality of power-efficient RISs integrated with the conventional network infrastructure.

This approach not only facilitates efficient analog self-interference cancellers but also allows more adaptable analog-to-digital (A/D) transmission and reception beamforming. Additionally, supervised and reinforcement learning techniques can be utilized for traffic prediction, enabling dynamic scheduling of uplink and downlink users in FD massive MIMO networks and reducing the overhead associated with multiple pilot-assisted channel estimates [3]. Extending this approach to efficient near-field beam tracking, machine learning could dynamically search over a time-evolving area of interest, enabling rapid adaptation to changing user positions and further optimizing resource allocation in complex, high-mobility scenarios.

Another promising direction for future work involves the development of advanced beam tracking algorithms tailored for mobile users (MUs). As MUs traverse through varying environments, maintaining optimal beam alignment becomes paramount for ensuring high-quality communication. This challenge necessitates real-time beam training, beamforming, and alignment, which must adapt dynamically to the changing positions and orientations of users. The complexities of this task arise from several factors, including the need for rapid adjustments to compensate for user movement, variations in channel conditions, and potential interference from surrounding obstacles. Moreover, achieving low-latency responses while ensuring high accuracy in beam alignment poses significant technical hurdles that could impact user experience. Despite these challenges, the growing importance of mobility in wireless communications—particularly in applications like autonomous vehicles, augmented reality, and IoT devices—underscores the necessity of such investigations. By addressing these complexities, we can significantly enhance user experience and system reliability in mobile environments, ensuring that users remain connected even in challenging circumstances.

Additionally, future work could focus on the real-world implementation of RIS technology, particularly addressing hardware challenges and ensuring compatibility with existing 5G networks. The transition from simulation to practical deployment will require addressing issues such as power consumption, form factor, and integration with existing communication infrastructure. Expanding the application of RIS to other environments, such as rural or large-scale outdoor networks, would also provide valuable insights into its broader utility and effectiveness. These applications could help bridge connectivity gaps in under-

served areas, enhancing communication capabilities and providing equitable access to high-speed data.

Finally, investigating the role of RIS in emerging communication technologies, including 6G and THz networks, could open new opportunities for low-latency, high-capacity wireless communication. As the demand for faster and more reliable connections continues to grow, RIS technology may play a crucial role in meeting these needs, particularly in supporting high-density urban areas and facilitating new applications such as holographic communication and immersive virtual experiences. Understanding how RIS can be effectively integrated into these next-generation networks will be essential for realizing the full potential of future wireless communication systems.

In conclusion, the exploration of RIS technology and its applications in beam management systems is paving the way for the future of wireless communications. As we continue to refine these approaches and tackle emerging challenges, we can unlock the full potential of RIS-enabled networks, ultimately enabling a new era of connectivity characterized by improved performance, efficiency, and user experience. The advancements in this field hold great promise for transforming how we interact with technology and connect with one another in an increasingly digital world.

ABBREVIATIONS - ACRONYMS

6G	Sixth-Generation Wireless Technology
A/D	Analog-to-Digital
ANN	Artificial Neural Network
AoA	Angle of Arrival
AoD	Angle of Departure
AP	Access Point
AWGN	Additive White Gaussian Noise
BA	Beam Alignment
BER	Bit Error Rate
BF	Beamforming
BS	Base Station
CAP	Continuous-Aperture
CE	Channel Estimation
CS	Compressed Sensing
CSI	Channel State Information
dB	Decibel
ELLA	Extremely Large-Scale Antenna Array
EM	Electromagnetic
ETSI	European Telecommunications Standards Institute
FD	Full-Duplex
FFT	Fast Fourier Transform
FoV	Field of View
IoT	Internet of Things
ISAC	Integrated Sensing and Communications
LoS	Line-of-Sight
MIMO	Multiple-Input Multiple-Output
mmWave	Millimeter-Wave
MU	Mobile User
NFC	Near-Field Communication

NLoS	Non-Line-of-Sight
PBIT	Passive Beamforming and Information Transfer
QoS	Quality of Service
RF	Radio Frequency
RIS	Reconfigurable Intelligent Surface
RPM	Reflection Pattern Modulation
RRA	Relative Reflection Angle
SISO	Single-Input Single-Output
SNR	Signal-to-Noise Ratio
THz	Terahertz Frequency

REFERENCES

[1] Mustafa Riza Akdeniz, Yuanpeng Liu, Shu Sun, Sundeep Rangan, Theodore S. Rappaport, and Elza Erkip. Millimeter wave channel modeling and cellular capacity evaluation. *arXiv preprint:1312.4921*, 2013.

[2] George C. Alexandropoulos. Position aided beam alignment for millimeter wave backhaul systems with large phased arrays. In *Proc. IEEE 7th International Workshop on Computational Advances in Multi-Sensor Adaptive Processing (CAMSAP)*, pages 1–5, 2017.

[3] George C. Alexandropoulos, Md Atiqul Islam, and Besma Smida. Full-duplex massive multiple-input, multiple-output architectures: Recent advances, applications, and future directions. *IEEE Vehicular Technology Magazine*, 17(4):83–91, 2022.

[4] George C. Alexandropoulos, Vahid Jamali, Robert Schober, and H. Vincent Poor. Near-field hierarchical beam management for RIS-enabled millimeter wave multi-antenna systems. In *Proc. IEEE 12th Sensor Array and Multichannel Signal Processing Workshop (SAM)*, June 2022.

[5] George C. Alexandropoulos, Geoffroy Lerosey, Merouane Debbah, and Mathias Fink. Reconfigurable intelligent surfaces and metamaterials: The potential of wave propagation control for 6G wireless communications. *arXiv preprint:2006.11136*, 2020.

[6] George C. Alexandropoulos, Nir Shlezinger, Idban Alamzadeh, Mohammadreza F. Imani, Haiyang Zhang, and Yonina C. Eldar. Hybrid reconfigurable intelligent metasurfaces: Enabling simultaneous tunable reflections and sensing for 6G wireless communications. *IEEE Vehicular Technology Magazine*, 19(1), 2024.

[7] George C. Alexandropoulos, Ioanna Vinieratou, Mattia Rebato, Luca Rose, and Michele Zorzi. Uplink beam management for millimeter wave cellular MIMO systems with hybrid beamforming. In *Proc. IEEE Wireless Communications and Networking Conference (WCNC)*, 2021.

[8] Ertugrul Basar, George C. Alexandropoulos, Yuanwei Liu, Qingqing Wu, Shi Jin, Chau Yuen, Octavia A. Dobre, and Robert Schober. Reconfigurable intelligent surfaces for 6G: Emerging hardware architectures, applications, and open challenges. *IEEE Vehicular Technology Magazine*, 19(3), 2024.

[9] Mohamadreza Delbari, George C. Alexandropoulos, Robert Schober, and Vahid Jamali. Far- versus near-field RIS modeling and beam design. *arXiv preprint:2401.08237*, 2024.

[10] Moritz Garkisch, Vahid Jamali, and Marzieh Najafi. Low-overhead channel estimation for IRS-assisted systems. Master's thesis, Friedrich-Alexander-Universität Erlangen-Nürnberg, 2022. Master's Thesis.

[11] Panagiotis Gavriilidis and George C. Alexandropoulos. Near-field beam tracking with extremely large dynamic metasurface antennas. *arXiv preprint:2406.01488*, 2024.

[12] Robert W. Heath Jr and Angel Lozano. *Foundations of MIMO Communication*. Cambridge University Press, 2018.

[13] Yuqiang Heng and Jeffrey G. Andrews. Machine learning-assisted beam alignment for mmWave systems. In *Proc. IEEE Global Communications Conference (GLOBECOM)*, 2019.

[14] Chongwen Huang, Sha Hu, George C. Alexandropoulos, Alessio Zappone, Chau Yuen, Rui Zhang, Marco Di Renzo, and Merouane Debbah. Holographic mimo surfaces for 6g wireless networks: Opportunities, challenges, and trends. *IEEE Wireless Communications*, 27(5), 2020.

[15] Chongwen Huang, Alessio Zappone, George C. Alexandropoulos, Mérouane Debbah, and Chau Yuen. Reconfigurable intelligent surfaces for energy efficiency in wireless communication. *IEEE Transactions on Wireless Communications*, 18(8), 2019.

[16] Vahid Jamali, George C. Alexandropoulos, Robert Schober, and H. Vincent Poor. Low-to-zero-overhead IRS reconfiguration: Decoupling illumination and channel estimation. *arXiv preprint:2111.09421*, 2021.

[17] Vahid Jamali, Marzieh Najafi, Robert Schober, and H. Vincent Poor. Power efficiency, overhead, and complexity tradeoff of IRS codebook design—quadratic phase-shift profile. *IEEE Communications Letters*, 25(6), 2021.

[18] Mengnan Jian, George C. Alexandropoulos, Ertugrul Basar, Chongwen Huang, Ruiqi Liu, Yuanwei Liu, and Chau Yuen. Reconfigurable intelligent surfaces for wireless communications: Overview of hardware designs, channel models, and estimation techniques. *Intelligent and Converged Networks*, 3(1), 2022.

[19] Shaoe Lin, Beixiong Zheng, George C. Alexandropoulos, Miaowen Wen, Marco Di Renzo, and Fangjiong Chen. Reconfigurable intelligent surfaces with reflection pattern modulation: Beamforming design and performance analysis. *IEEE Transactions on Wireless Communications*, 20(2), 2021.

[20] Ruiqi Liu, Shuang Zheng, Qingqing Wu, Yifan Jiang, Nan Zhang, Yuanwei Liu, Marco Di Renzo, and George C. Alexandropoulos. Sustainable wireless networks via reconfigurable intelligent surfaces (RISs): Overview of the ETSI ISG RIS. *arXiv preprint:2406.05647*, 2024.

[21] Yuanwei Liu, Zhaolin Wang, Jiaqi Xu, Chongjun Ouyang, Xidong Mu, and Robert Schober. Near-field communications: A tutorial review. *IEEE Open Journal of the Communications Society*, 4, 2023.

[22] Antonino Masaracchia, Dang Van Huynh, George C. Alexandropoulos, Berk Canberk, Octavia A. Dobre, and Trung Q. Duong. Toward the metaverse realization in 6G: Orchestration of RIS-enabled smart wireless environments via digital twins. *IEEE Internet of Things Magazine*, 7(2), 2024.

[23] Weidong Mei, Beixiong Zheng, Changsheng You, and Rui Zhang. Intelligent reflecting surface aided wireless networks: From single-reflection to multi-reflection design and optimization. *arXiv preprint:2109.13641*, abs/2109.13641, 2021.

[24] Deepak Mishra, George C. Alexandropoulos, and Swades De. Energy sustainable IoT with individual QoS constraints through miso swipt multicasting. *IEEE Internet of Things Journal*, 5(4), 2018.

[25] Moustafa Rahal, Benoit Denis, Kamran Keykhosravi, Musa Furkan Keskin, Bernard Uguen, George Alexandropoulos, and Henk Wymeersch. Performance of RIS-aided near-field localization under beams approximation from real hardware characterization. *EURASIP Journal on Wireless Communications and Networking*, 2023, 08 2023.

[26] Marco Di Renzo, Mérouane Debbah, Dinh Thuy Phan Huy, Alessio Zappone, Mohamed-Slim Alouini, Chau Yuen, Vincenzo Sciancalepore, George C. Alexandropoulos, Jakob Hoydis, Haris Gacanin, Julien de Rosny, Ahcène Bounceur, Geoffroy Lerosey, and Mathias Fink. Smart radio environments empowered by AI reconfigurable meta-surfaces: An idea whose time has come. *arXiv preprint:1903.08925*, 2019.

[27] Fabio Saggese, Victor Croisfelt, Radosław Kotaba, Kyriakos Stylianopoulos, George C. Alexandropoulos, and Petar Popovski. On the impact of control signaling in RIS-empowered wireless communications. *IEEE Open Journal of the Communications Society*, 5, 2024.

[28] R. S. Prasobh Sankar, Sundeep Prabhakar Chepuri, and Yonina C. Eldar. Beamforming in integrated sensing and communication systems with reconfigurable intelligent surfaces. *IEEE Transactions on Wireless Communications*, 23(5), 2024.

[29] Besma Smida, Ashutosh Sabharwal, Gábor Fodor, George C. Alexandropoulos, Himal A. Suraweera, and Chan-Byoung Chae. Full-duplex wireless for 6g: Progress brings new opportunities and challenges. *IEEE Journal on Selected Areas in Communications*, 41(9):2729–2750, 2023.

[30] Emilio Calvanese Strinati, George C. Alexandropoulos, Vincenzo Sciancalepore, Marco Di Renzo, Henk Wymeersch, Dinh-Thuy Phan-Huy, Maurizio Crozzoli, Raffaele D'Errico, Elisabeth De Carvalho, Petar Popovski, Paolo Di Lorenzo, Luca Bastianelli, Mathieu Belouar, Julien Etienne Mascolo, Gabriele Gradoni, Sendy Phang, Geoffroy Lerosey, and Benoît Denis. Wireless environment as a service enabled by reconfigurable intelligent surfaces: The RISE-6G perspective. In *Proc. Joint European Conference on Networks and Communications 6G Summit (EuCNC/6G Summit)*, 2021.

[31] Emilio Calvanese Strinati, George C. Alexandropoulos, Henk Wymeersch, Benoît Denis, Vincenzo Sciancalepore, Raffaele D'Errico, Antonio Clemente, Dinh-Thuy Phan-Huy, Elisabeth De Carvalho, and Petar Popovski. Reconfigurable, intelligent, and sustainable wireless environments for 6G smart connectivity. *IEEE Communications Magazine*, 59(10), 2021.

[32] Spyridon Vassilaras and George C. Alexandropoulos. Cooperative beamforming techniques for energy efficient IoT wireless communication. In *Proc. IEEE International Conference on Communications (ICC)*, 2017.

[33] Evangelos Vlachos, Aryan Kaushik, Yonina C. Eldar, and George C. Alexandropoulos. Time-domain channel estimation for extremely large MIMO THz communication systems under dual-wideband fading conditions. *arXiv preprint:2310.14745*, 2024.

[34] Peilan Wang, Jun Fang, Huiping Duan, and Hongbin Li. Compressed channel estimation for intelligent reflecting surface-assisted millimeter wave systems. *IEEE Signal Processing Letters*, 27, 2020.

[35] Peilan Wang, Jun Fang, Xiaojun Yuan, Zhi Chen, and Hongbin Li. Intelligent reflecting surface-assisted millimeter wave communications: Joint active and passive precoding design. *IEEE Transactions on Vehicular Technology*, 69(12), 2020.

[36] Peilan Wang, Jun Fang, Xiaojun Yuan, Zhi Chen, and Hongbin Li. Intelligent reflecting surface-assisted millimeter wave communications: Joint active and passive precoding design. *IEEE Transactions on Vehicular Technology*, 69(12), 2020.

[37] Peilan Wang, Jun Fang, Weizheng Zhang, Zhi Chen, Hongbin Li, and Wei Zhang. Beam training and alignment for RIS-assisted millimeter-wave systems: State of the art and beyond. *IEEE Wireless Communications*, 29(6), 2022.

[38] Zhenyu Xiao, Tong He, Pengfei Xia, and Xiang-Gen Xia. Hierarchical codebook design for beamforming training in millimeter-wave communication. *IEEE Transactions on Wireless Communications*, 15(5), 2016.

[39] Jie Xu, Li You, George C. Alexandropoulos, Xinping Yi, Wenjin Wang, and Xiqi Gao. Near-field wideband extremely large-scale MIMO transmissions with holographic metasurface-based antenna arrays. *IEEE Transactions on Wireless Communications*, 23(9), 2024.

[40] Changsheng You, Beixiong Zheng, and Rui Zhang. Fast beam training for IRS-assisted multiuser communications. *IEEE Wireless Communications Letters*, 9(11), 2020.